

Beam size measurement with gratings at BEPCII



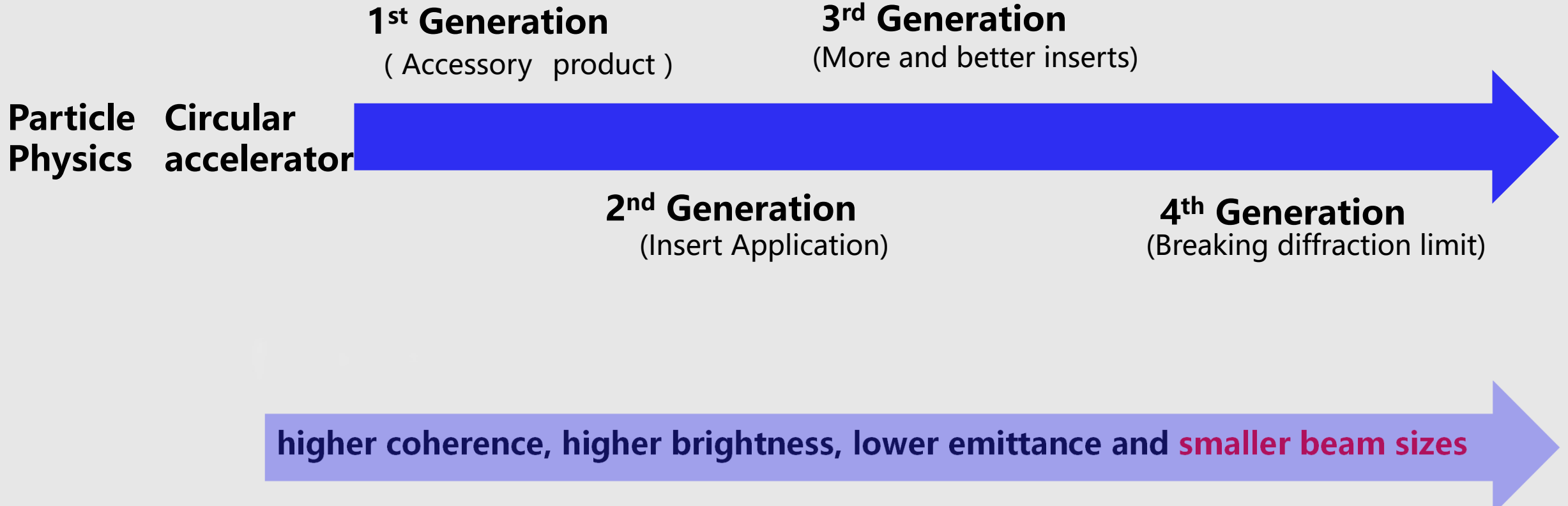
Zhang Wan

2024-09-10

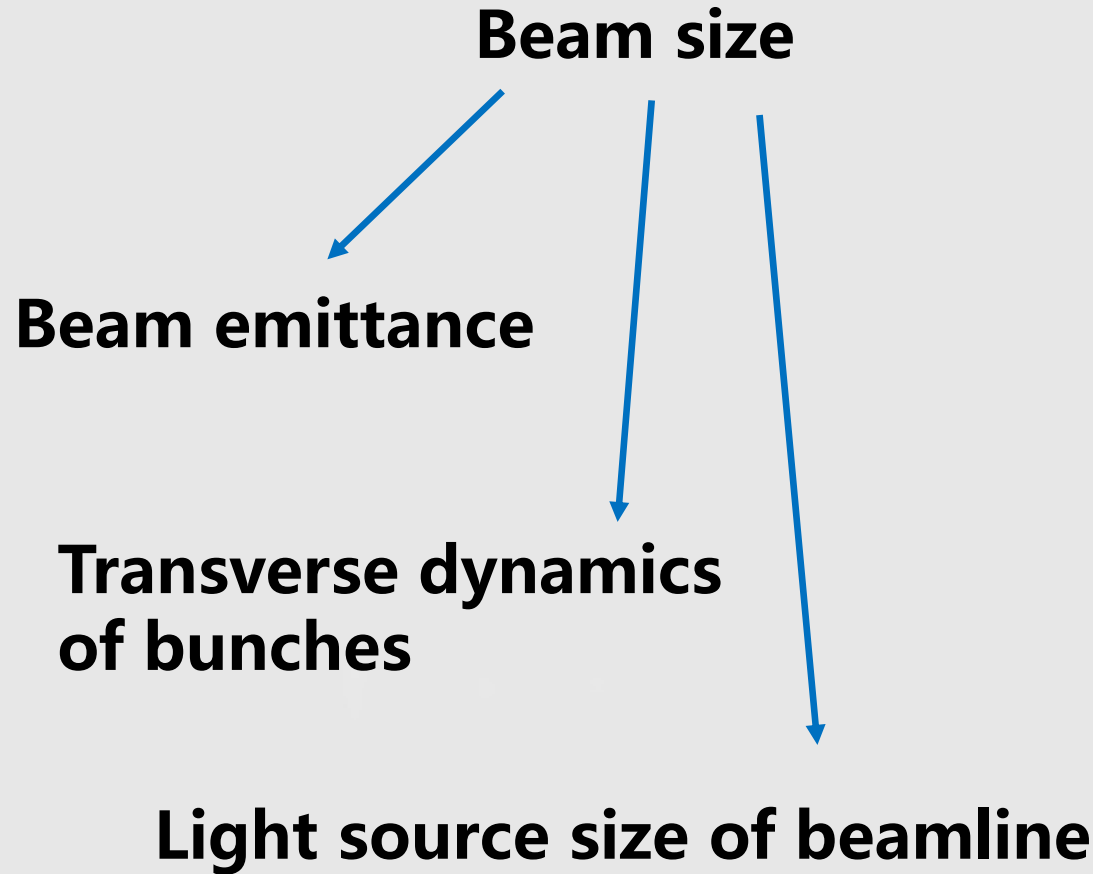
Contents

- **Background**
- **Theory**
- **Setup**
- **Results**
- **Potential**

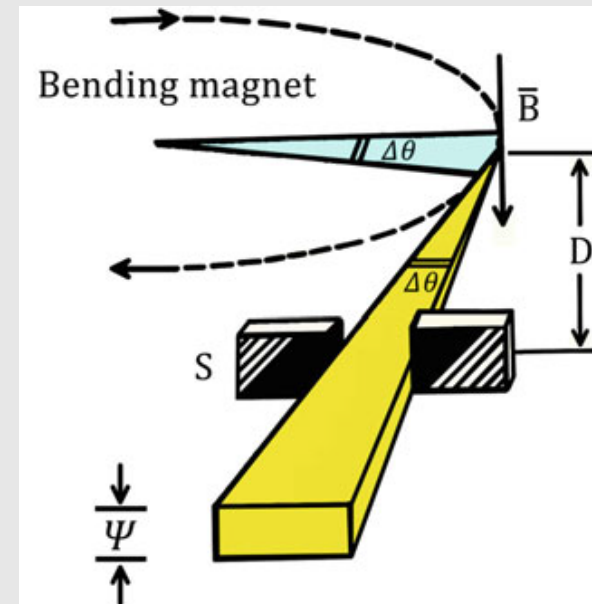
Background



Background



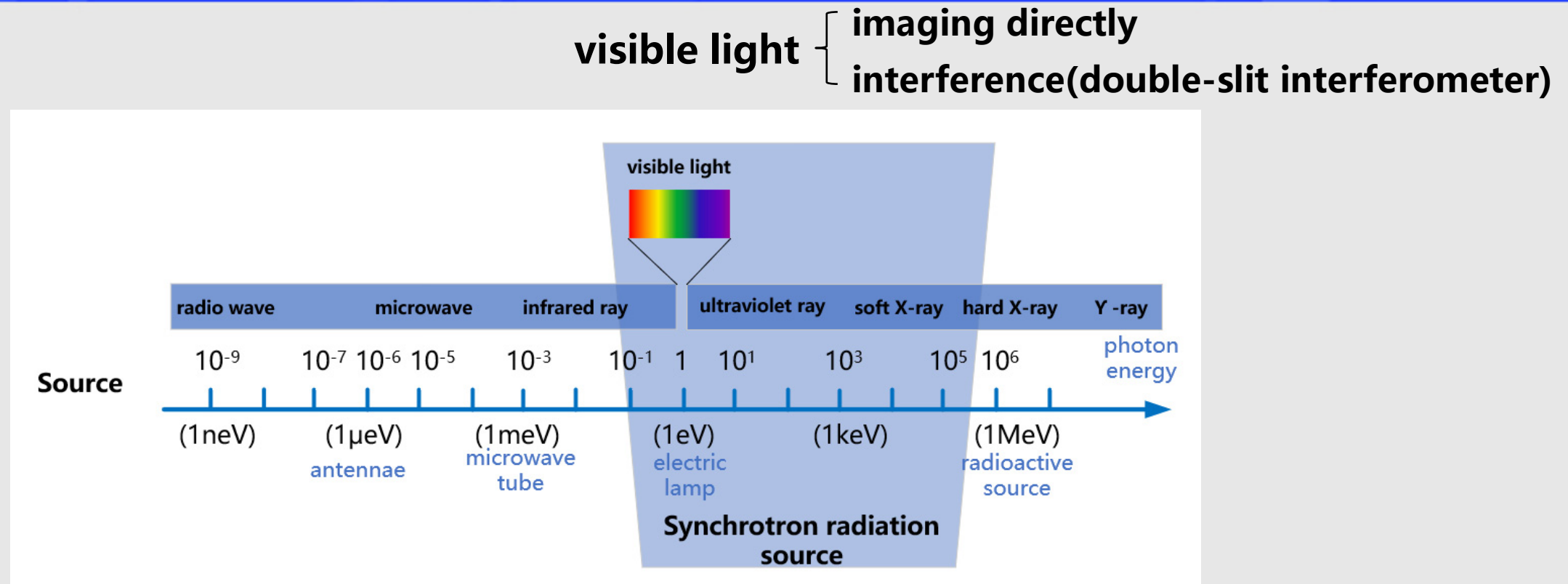
Beam size measurement



Synchrotron light

(unstoppable, natural photo isolation,
the light source size is almost equal to the
beam size)

Background



short wavelength
high resolution

X-ray { pinhole imaging
focused imaging
(KB mirror, CRL, FZP)
• • •

Background

Method by using X-ray

Methods	X-ray pinhole imaging	X-ray double-slit interferometer	X-ray focused imaging (KB mirror, CRL, FZP)	Grating Talbot effect
optical device	simple	complex	complex	simple
Measuring Direction	Any direction	One direction	Any direction	Any direction
real-time measurement	Yes	Yes	Yes	No
Measurable beam size (μm)	>10 μm	about 5 μm	about 5 μm	<5 μm

Background

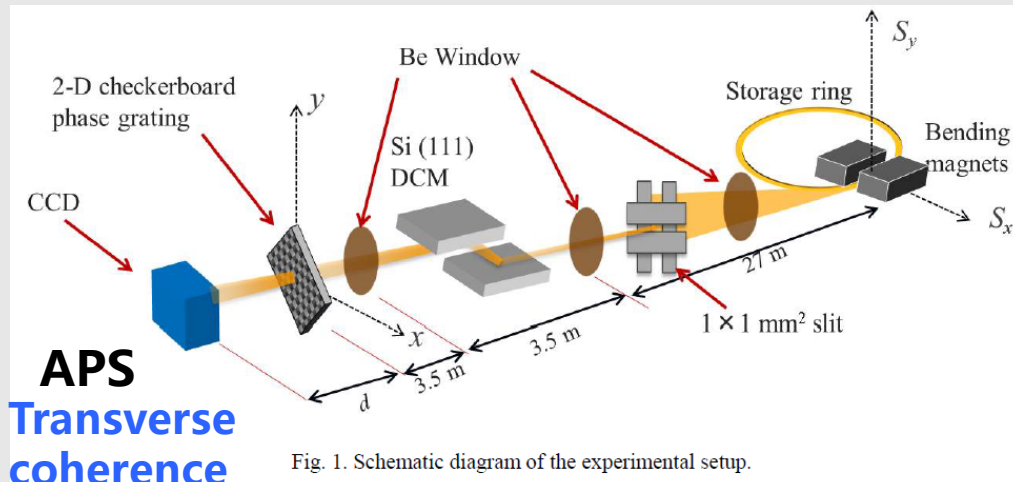
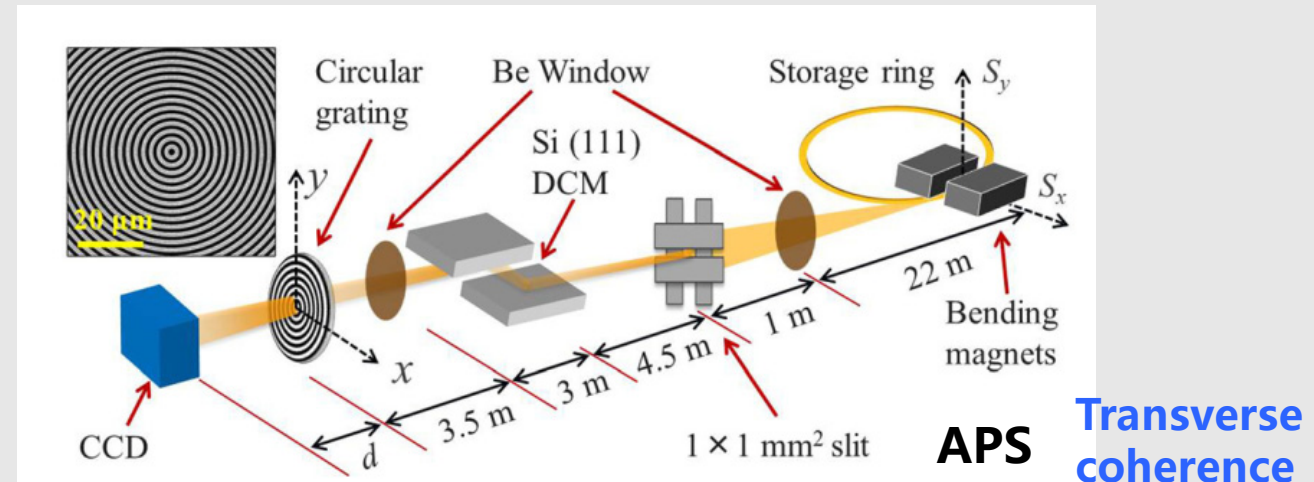
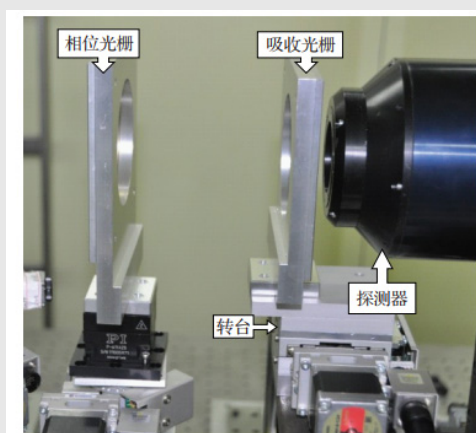
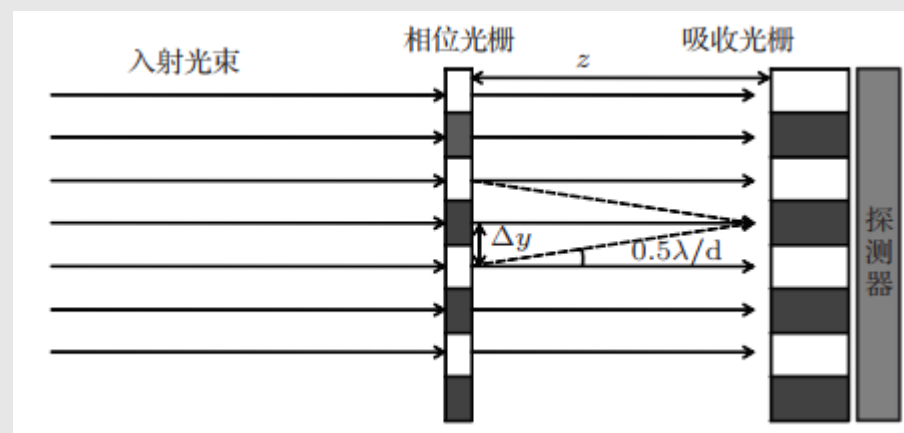


Fig. 1. Schematic diagram of the experimental setup.



*Shi X et al. Applied Physics Letters, 2014, 105(4): 041116.



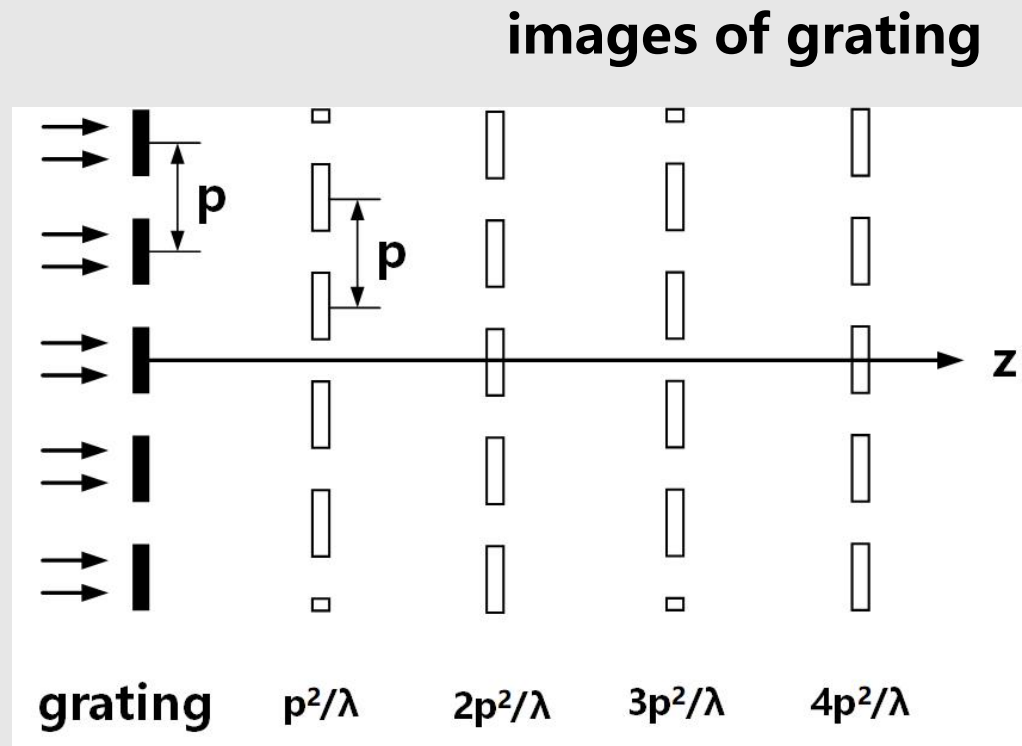
SSRF
(33keV,
measured:23 μm ,
theoretical :22 μm)

*Qi JC et al. Acta Phys. Sin. 2014, 63(10): 104202.

Theory

Grating Talbot effect

Monochromatic light

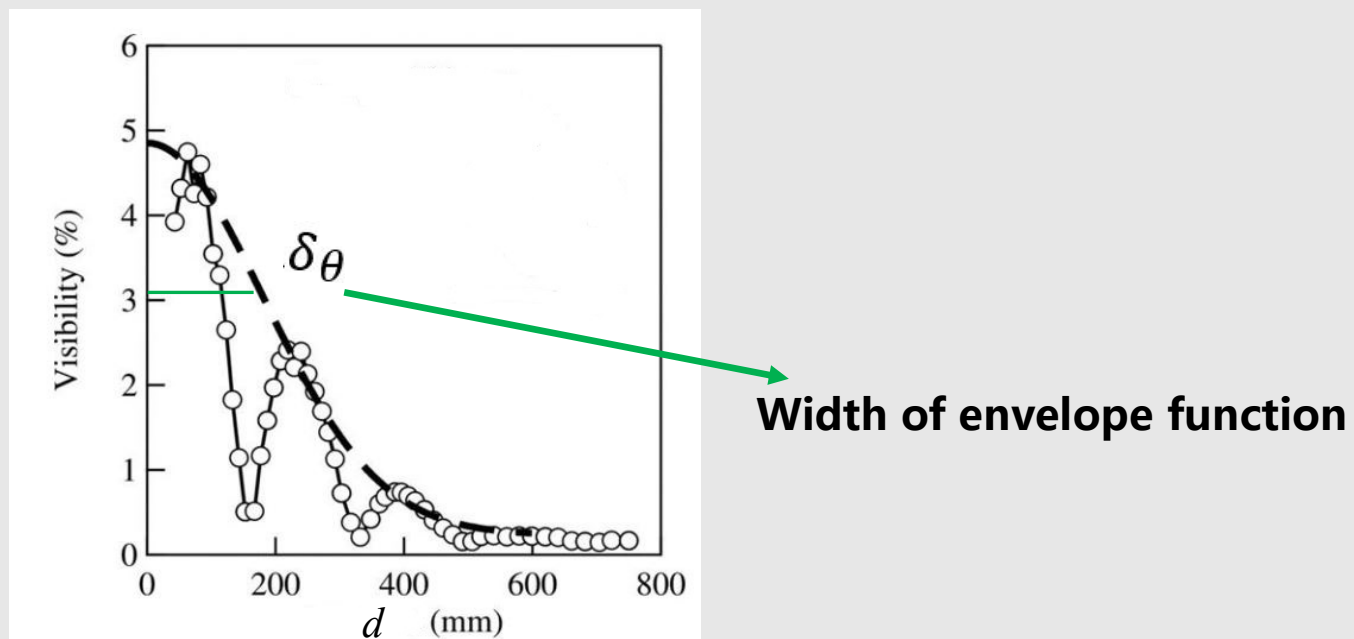
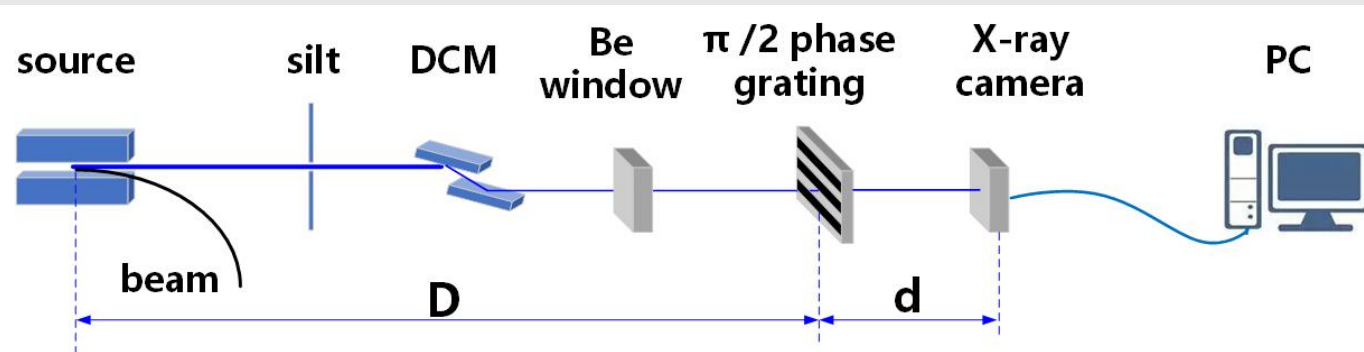


p is grating period, λ is the transmission wavelength

Completely coherent light source → Visibilities of images are equal

Partially coherent light source → Visibility decreases with the increase of transmission distance → spatial coherence

Theory



distance from source to grating

$$\xi_x = \frac{\lambda D}{2\pi\sigma_x}, \quad \xi_y = \frac{\lambda D}{2\pi\sigma_y}$$

spatial coherence length

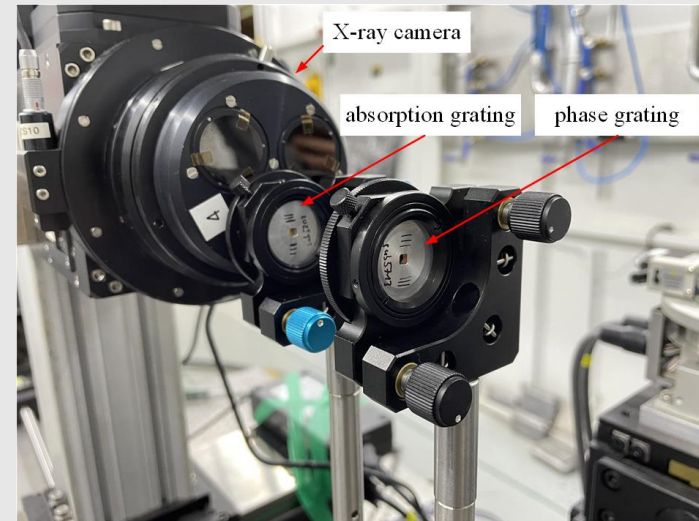
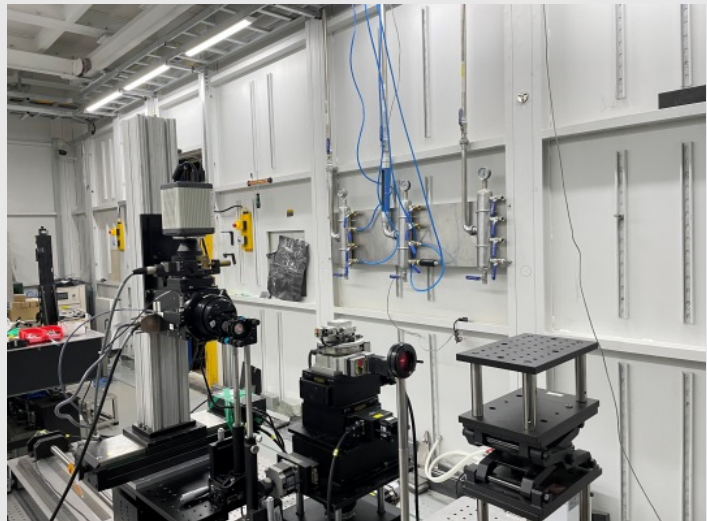
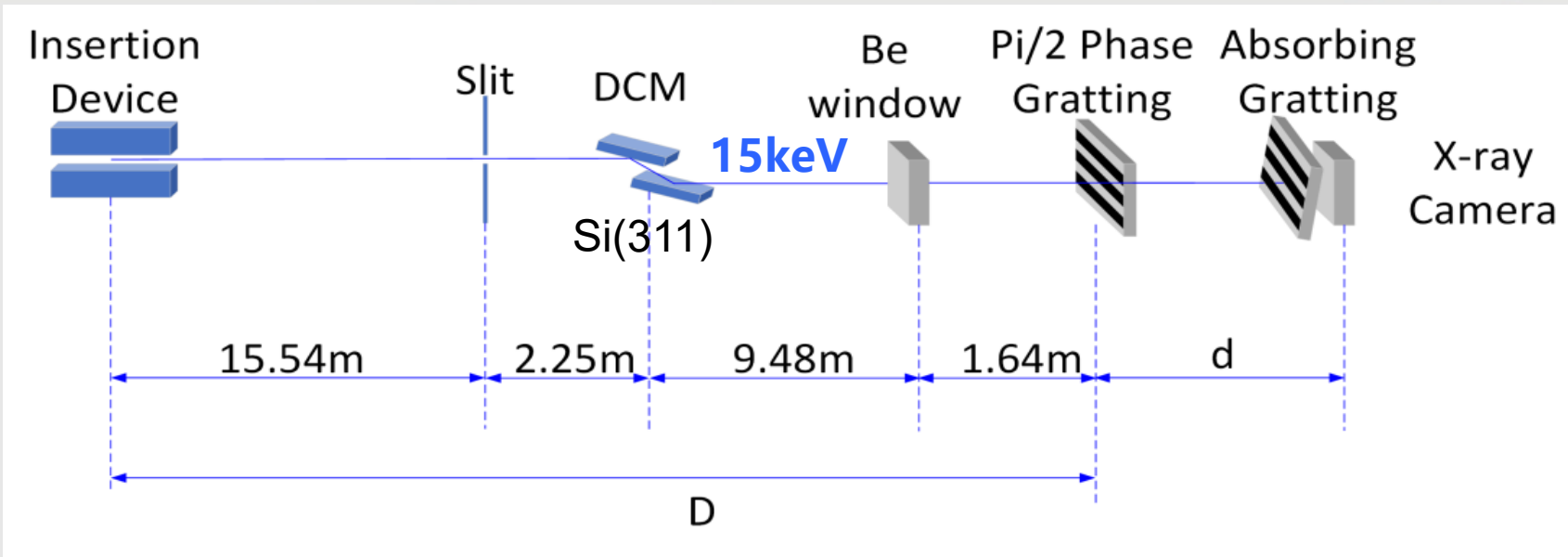
source size

$$\xi_{exp,\theta} = \frac{\lambda\delta_\theta}{p_\theta}$$

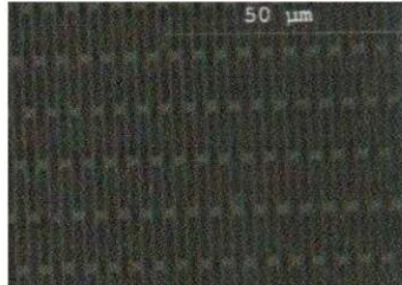
period of grating image

$$\sigma_x = \frac{p_x D}{2\pi\delta_x}, \quad \sigma_y = \frac{p_y D}{2\pi\delta_y}$$

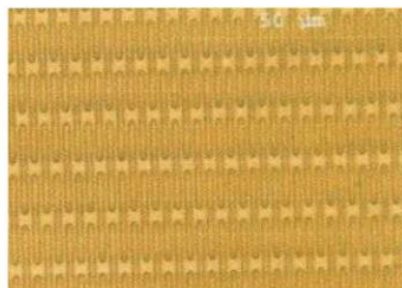
Setup



Setup



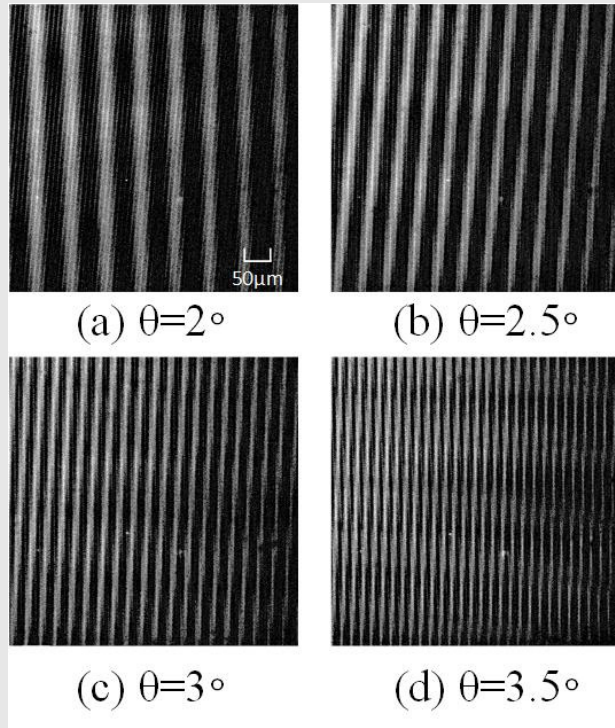
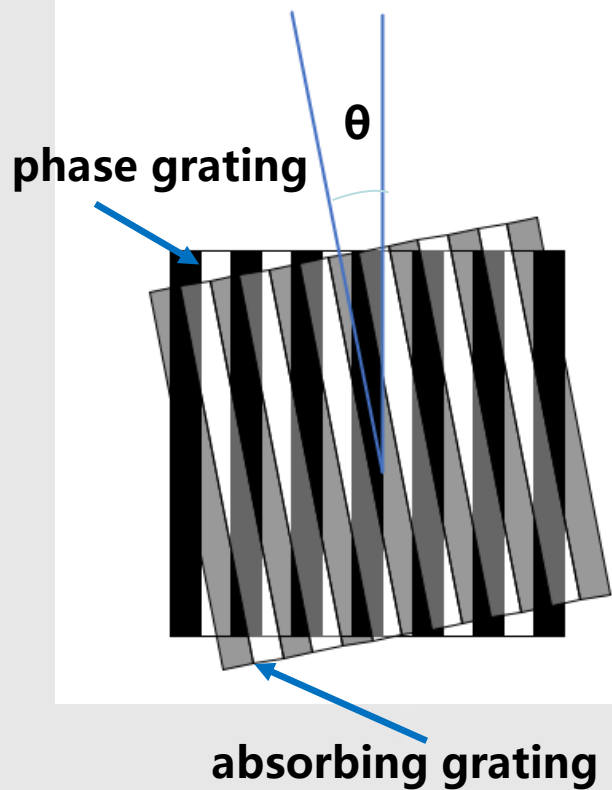
(a) phase grating



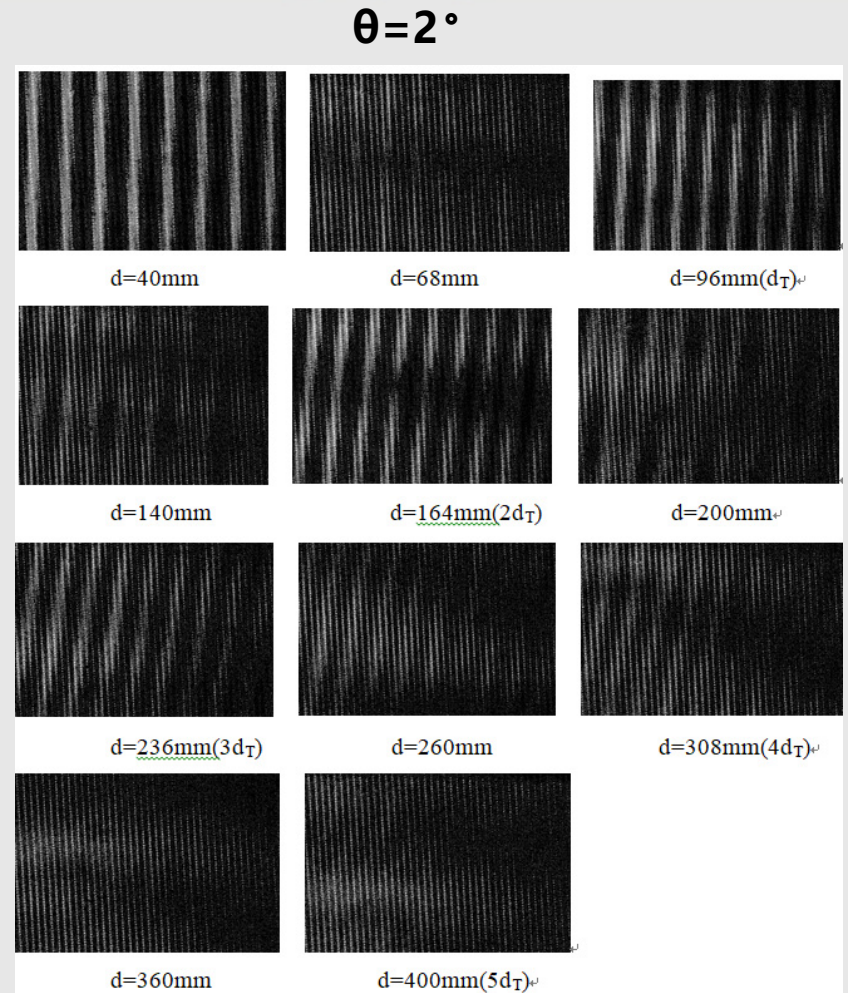
(b) absorption grating

Parameters	phase grating	absorption grating
Period	2.4μm	2.4μm
Duty Cycle	0.53±0.01	0.51±0.01
Area	>2.5×2.5mm ²	>2.5×2.5mm ²
Height	Polymer 18.6μm	Gold 14±1μm
Substrate	10μm Polyimide	10μm Polyimide

Results

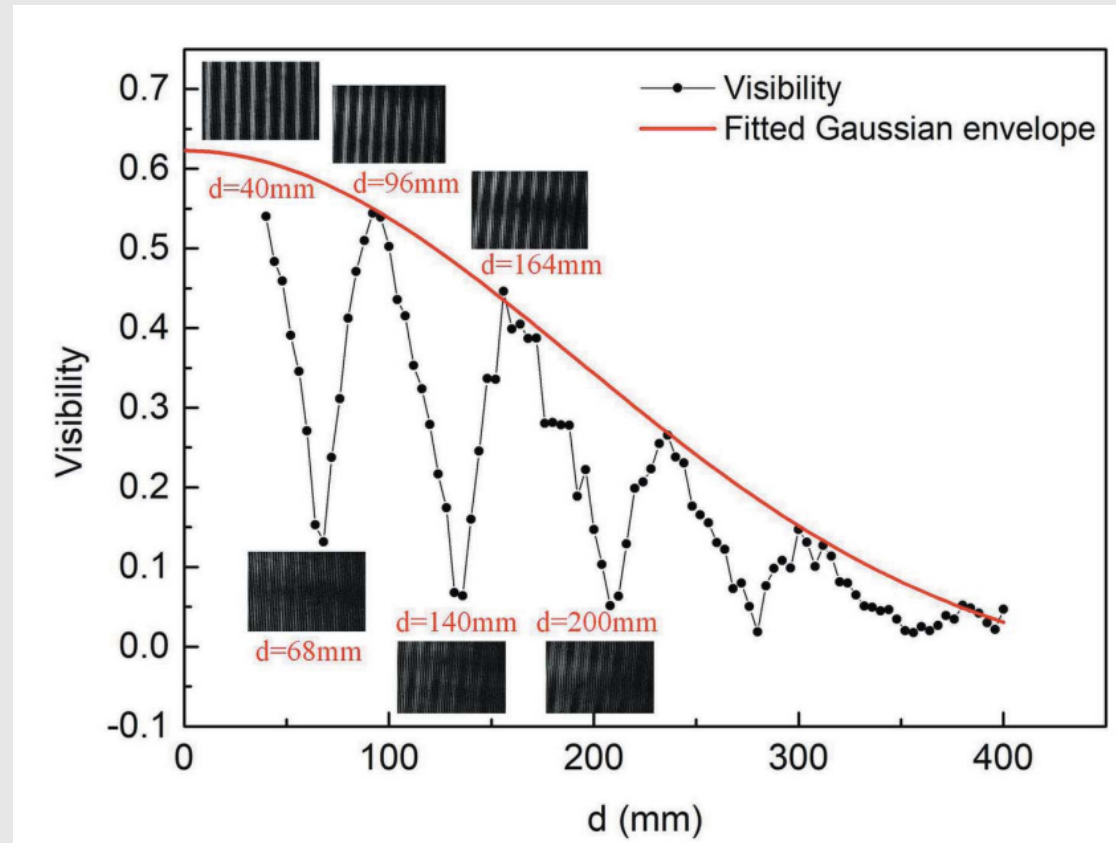


Moire fringe images

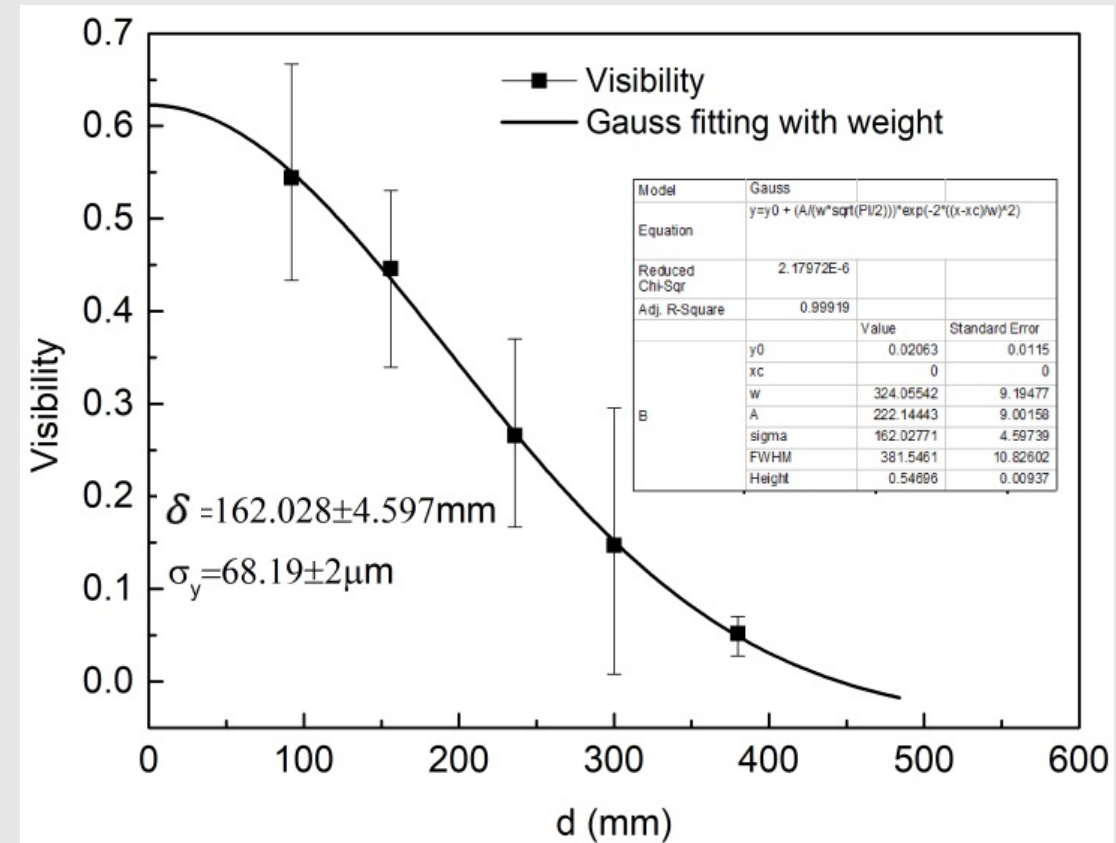


The interference images at different Talbot distances

Results



The visibility shows periodic oscillations.
The local maximum of visibility at fractional Talbot distance decreases gradually due to the partial coherence of the source.

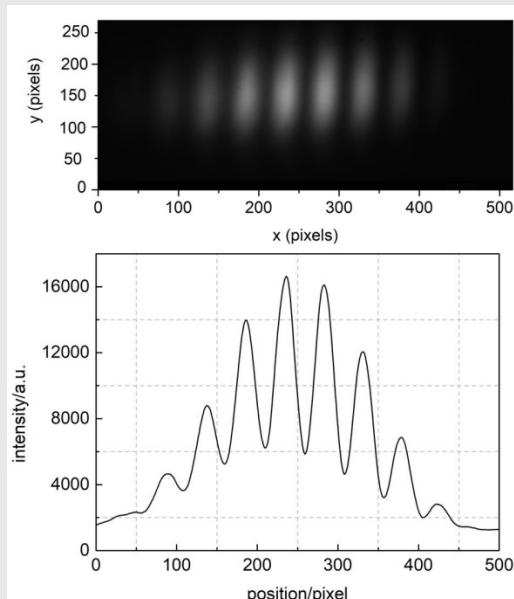
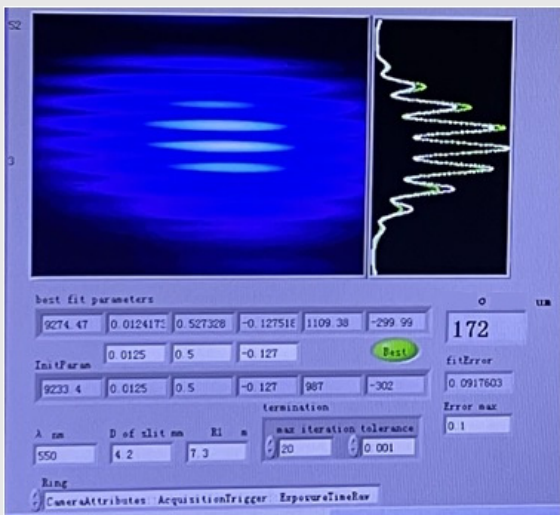


spatial coherence length $\xi_y = 5.592\mu\text{m}$
source size $\sigma_y = 68.19\mu\text{m}$

Results

contrast experiment

The visible light beamline of BEPCII



the vertical beam size measurement with a double-slit interferometer

The comparison of vertical emittance derived from two methods

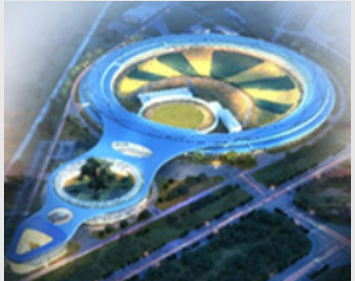
$$\sigma_y^2 = \varepsilon_y \beta_y$$

Parameters	3W1	visible light beamline
Method	grating self-imaging	visible light imaging
β_y	3.2877m	20.975m
σ_y	68.19μm	171.4μm
ε_y	1.41nm·rad	1.40nm·rad

The results of the two methods agree very well

Potential

4th Generation



higher coherence

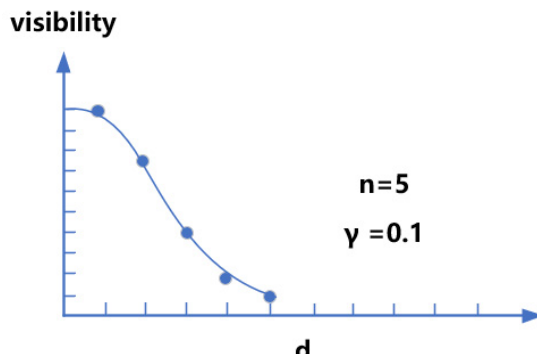
lower emittance

smaller beam size

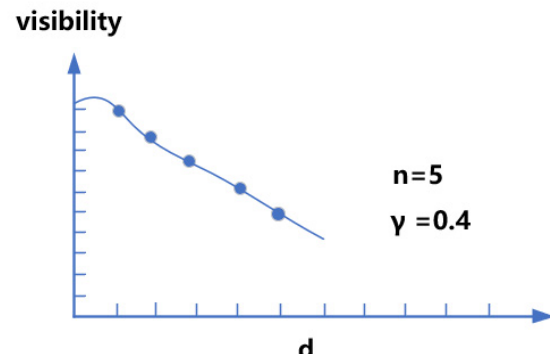
$$\sqrt{\frac{2 \ln \gamma}{n(1-n)}} \xi_\theta < p_\theta < \left(\frac{2 \lambda d_{max}}{2n-1} \right)^{1/2}$$

HEPS

stores ring physical parameters	value	unit
linear section with high β		
Beam size in horizontal direction/ and vertical direction(rms)	16.7/5.1	μm
beam divergence angle in horizontal direction/ and vertical direction(rms)	1.65/0.53	μrad



Suitable n ($n>5$)



Suitable $\gamma = V_{min}/V_{max}$

The suitable grating period can be derived according to various conditions.

References

- [1] D. K. Pogoreliy et al., "Real-time phase-contrast imaging at the Kurchatov synchrotron radiation source" , Nucl. Instrum. Methods, vol. 603, pp. 167-169, 2009. doi: 10.1016/j.nima.2008.12.146
- [2] W. Yang et al., "Coherent diffraction imaging of nanoscale strain evolution in a single crystal under high pressure" , Nat. Commun., vol. 4, p. 1680, 2013. doi:10.1038/ncomms2661
- [3] A. Sakdinawat and D. Attwood, "Nanoscale X-ray imaging" , Nat. Photonics, vol. 4, no. 12, pp. 840–848, 2010. doi:10.1038/nphoton.2010.267
- [4] A. D. Garg et al., "Design of synchrotron radiation interfer-ometer (SRI) for beam size measurement at visible diagnos-tics beamline in Indus-2 SRS" , Nucl. Instrum. Methods, vol. 902, pp. 164-172, 2018. doi:10.1016/j.nima.2018.06.024
- [5] T. Mitsuhashi, "Beam profile and size measurement by SR interferometers" , in: Proceedings of the Joint US–CERN–Japan–Russia School on Particle Accelerators, World Scien-tific, Montreux and Geneva, Switzerland, 1999, pp. 399–427. doi: 10.1142/9789812818003_0018
- [6] C. Thomas, G. Rehm, and I. Martin, "X-ray pinhole camera resolution and emittance measurement" , Phys. Rev. Spec. Top-AC., vol. 13, no. 022805, 2010. doi: 10.1103/PhysRevSTAB.13.022805
- [7] A. Garg et al., "Design of x-ray diagnostic beamline for a synchrotron radiation source and measurement results" , Nucl. Instrum. Methods Phys. Res. A, vol. 754, pp. 15-23, 2014. doi:10.1016/j.nima.2014.04.013
- [8] W. Leitenberger et al., "Double pinhole diffraction of white synchrotron radiation" , Physica B, vol. 336, pp. 63–67, 2003. doi: 10.1016/S0921-4526(03)00270-9
- [9] Y. Suzuki et al., "X-ray microbeam with sputtered-sliced Fresnel zone plate at SPring-8 undulator beamline" , Nucl. Instrum. Methods, vol. 467, pp. 951-953, 2001. doi: 10.1016/S0168-9002(01)00532-0
- [10] A. Alatas et al., "Improved focusing capability for inelastic X-ray spectrometer at 3-ID of the APS: A combina-tion of toroidal and Kirkpatrick-Baez (KB) mirrors" , Nucl. Instrum. Methods, vol. 649, pp. 166-168, 2011. doi: 10.1016/j.nima.2010.11.068

References

- [11] N. Samadi, X. Shi, L. Dallinc and D. Chapman, "A real-time phase-space beam emittance monitoring system" , J. Synchrotron Rad., vol. 26, pp. 1213–1219, 2019. doi: 10.1107/S1600577519005423
- [12] Y. Kagoshima et al., "Measurement of the horizontal beam emittance of undulator radiation by tandem-double-slit optical system" , J. Synchrotron Rad., vol. 27, pp. 799–803, 2020. doi: 10.1107/S1600577520004415
- [13] S. Marathe et al., "Probing transverse coherence of x-ray beam with 2-D phase grating interferometer" , Optics Ex-press, vol. 22, pp. 14041-14053, 2014. doi: 10.1364/oe.22.014041
- [14] X. Shi et al., "Circular grating interferometer for map-ping transverse coherence area of X-ray beams" , Appl. Phys. Lett., vol. 105, p. 041116, 2014. doi: 10.1063/1.4892002
- [15] M. Born and E. Wolf, "Principles of Optics" , 7th ed. University Press, Cambridge, 1999.
- [16] P. Cloetens, J. P. Guigay, C. De Martino, J. Baruchel, and M. Schlenker, "Fractional Talbot imaging of phase grat-ings with hard x rays" , Opt. Lett., vol. 22, pp. 1059–1061, 1997. doi: 10.1364/OL.22.001059
- [17] J. P. Guigay, S. Zabler, P. Cloetens, C. David, R. Mok-so, and M. Schlenker, "The partial Talbot effect and its use in measuring the coherence of synchrotron X-rays" , J. Synchro-tron Radiat. Vol. 11, no.6, pp. 476–482, 2004.
doi:10.1107/S0909049504024811
- [18] F. Pfeiffer et al., "Shearing interferometer for quantify-ing the coherence of hard X-ray beams" , Phys. Rev. Lett., vol. 94, no. 16, p. 164801, 2005. doi: 10.1103/PhysRevLett.94.164801
- [19] I. Zanette, C. David, S. Rutishauser, and T. Weitkamp, "2D grating simulation for X-ray phase-contrast and dark-field imaging with a Talbot interferometer" , in X-Ray Optics and Microanalysis, Proceedings of the 20th International Congress, CP1221, M. Denecke and C. Walker, eds. (Ameri-can Institute of Physics, pp. 73–79, 2010.

Thank you very much !